Inorganic Chemistry

Article

pubs.acs.org/IC

Biologically Compatible, Phosphorescent Dimetallic Rhenium Complexes Linked through Functionalized Alkyl Chains: Syntheses, Spectroscopic Properties, and Applications in Imaging Microscopy

Rebeca G. Balasingham,[†] Flora L. Thorp-Greenwood,[†] Catrin F. Williams,[‡] Michael P. Coogan,*[,†] and Simon J. A. Pope*[,†]

[†]School of Chemistry and [‡]School of Biosciences, Main Building, Cardiff University, Cardiff CF10 3AT, Cymru/Wales, U.K.

ABSTRACT: A range of luminescent, dimetallic complexes based upon the rhenium *fac*-tricarbonyl diimine core, linked by aliphatic chains of varying lengths and functionality, have been synthesized and their photophysical properties examined. Each complex displays characteristic $^3M_{Re}L_{diimine}CT$ emission in aerated acetonitrile solution, with long lifetimes in the range of 129−248 ns and corresponding quantum yields in the range 3.2−8.0%. In aqueous solution, as opposed to acetonitrile, the complexes generally show a small hypsochromic shift in λ_{em} and an extension of the ^{3}MLCT lifetime, attributed to a hydrophobically driven association of the alkyl chains with the rhenium-bound diimine units. In live cell imaging experiments using MCF7 cells the complexes all show good uptake by non-energy dependent mechanisms without endosomal entrainment, and with varying propensity to localize in organelles. The degrees of uptake and localization properties are discussed in terms of the length and chemical nature of the linkers, and in terms of the likely interactions between these and the various cellular components encountered.

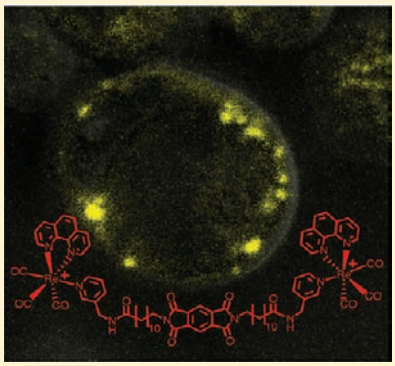

INTRODUCTION

Luminescent diimine derivatives of the *fac*-{$Re^I(CO)_3$} core have been known as efficient emitters for many years, and their photophysical properties widely studied.[1−5] In recent years they have become recognized as valuable luminophores for application in live cell imaging studies through confocal fluorescence microscopy.[6−12] Such complexes can be functionalized in a stepwise manner allowing a number of physical features to be tuned separately, with the possibility of combining variations in the diimine fragment and the axial ligands to give a large range of related systems, and offer many attractive features in the design of cell imaging agents.[6] These attractive features include: aqueous stability; low intrinsic cytotoxicity (due to the kinetically inert d^6 electronic structure impeding ligand exchange and associated heavy-metal toxicity); cationic charge and lipophilicity, which assists in crossing bilipid membranes, and accumulation inside cells with healthy membrane potential; and their attractive photophysical properties.[6] Visible wavelength excitation and detection are possible through the formation of a long-lived ^{3}MLCT excited state which makes complexes of this nature attractive for imaging applications. By comparison with the typical organic fluorophores they have large Stokes' shifts and long luminescence lifetimes, which can assist in differentiating their emission from autofluorescence emanating from endogenous material by wavelength filtering or time gating (recently demonstrated in cell work with a related d^6 Ir^{III} complex),[13−19] leading to an improved signal-to-background ratio.[20] Such is the utility of these complexes that organelle specificity has been demonstrated through targeting vectors and tuned functionality, and examples of rhenium-based agents now exist which can target most of the important cellular organelles.[21,22]

The vast majority of the previous studies have, however, focused exclusively upon functionalized monometallic complexes and/or relatively small molecular weight complexes. In this study, we present the possibilities afforded through larger, lipophilic dimetallic rhenium species, which, because of their dicationic nature, may show enhanced accumulation in healthy cells over the monocationic analogues. The internal membranes of certain organelles (including mitochondria) also have membrane potentials, which would encourage the accumulation of dicationic species over monocationic variants. As the rate of membrane diffusion could also be expected to suffer as a function of size (Fick's law), the complexes are designed with lipophilicity in mind to enhance permeancy. As it has previously been noted that related lipophilic complexes show unusual modulation of luminescence in aqueous media,[23] because of hydrophobically driven intramolecular interactions between alkyl chains and diimine ligands, an investigation of the comparative photophysical behavior of the complexes in organic solvent and water has also been undertaken.

EXPERIMENTAL SECTION

General Measurements and Analysis. All photophysical data were obtained on a JobinYvon-Horiba Fluorolog spectrometer fitted with a JY TBX picosecond photodetection module. Luminescence lifetimes were obtained using either 295 or 372 nm nanoLEDs

Received: August 1, 2011
Published: January 20, 2012

   dx.doi.org/10.1021/ic201654d | *Inorg. Chem.* 2012, 51, 1419−1426

operating at 1 MHz. All lifetime data were collected using the JY-Horiba FluoroHub single photon counting module in multichannel scaler mode. Lifetimes were obtained using the provided software, DAS6. IR spectra were recorded on a Varian 7000 FT-IR. LR Mass spectra were obtained using a Bruker MicroTOF LC. UV−vis data were recorded as solutions on a Jasco 570 spectrophotometer. ^{1}H and ^{13}C{^{1}H} NMR spectra were run either on a NMR-FT Bruker 250 or 400 MHz spectrometers and obtained using $CDCl_3$, CD_3OD, or CD_3CN solutions; ^{1}H NMR chemical shifts (δ) were determined relative to internal $Si(CH_3)_4$ and are given in parts per million (ppm). Elemental analyses were conducted by Medac Ltd. (U.K.).

Human Cell Incubation Studies. Human adenocarcinoma cells (MCF-7), obtained from the European Collection of Cell Cultures, Porton Down, Wiltshire, U.K., were maintained in Hepes modified minimum essential medium (HMEM) supplemented with 10% fetal bovine serum, penicillin, and streptomycin. Cells were detached from the plastic flask using trypsin−EDTA solution, and suspended in an excess volume of growth medium. The homogeneous cell suspension was then distributed into 1 mL aliquots with each aliquot being subject to incubation with the complexes final concentration 50 μg mL^{-1}, at 4 °C for 30 min. Cells were finally washed three times in phosphate buffer saline (PBS, pH 7.2), harvested by centrifugation (5 min, 800 g), and mounted on a slide for imaging. Preparations were viewed using a Leica TCS SP2 AOBS confocal laser microscope using X63 objective, with excitation at 405 nm and detection at 510−580 nm. Z-plane slices were used to record multiple single-plane views cell populations to estimate percentage uptake of lumophores.

Co-Localization/Nucleolar Staining Experiments. MCF-7 adenocarcinoma cells were harvested as indicated above, resuspended in HMEM, and incubated with both complex (final concentration 50 μg mL^{-1}) and the nucleolar-specific stain SYTORNASelect (final concentration 250 μM) for 1.5 h at 4 °C. Cells were then washed three times in PBS, mounted, and viewed as above by confocal microscopy. The excitation and detection wavelengths used for imaging were ex. 405 nm, em. 510−580 nm for complex, and ex. 488 nm, det. 520−540 nm for SYTORNASelect.

Toxicity Analyses of the Rhenium Complexes on MCF-7 Cells. Complexes were incubated with MCF-7s for 1.5 h incubation at a concentration of 50 μg/mL. After incubation, cells were washed and incubated with 0.5 μg/mL propidium iodide for 30 min and the number of nonviable cells (PI-stained) counted. Control (DMSO only), 3 (± 2.92 SD)% dead cells; **Re2-phen-L3**, 7 (± 4.66 SD) % dead cells; **Re2-phen-L2**: 1 (± 1.79) % dead cells; **Re2-bipy-L5**: 4 (± 3.51) % dead cells (SD = standard deviation of 5 different counts).

Materials and Procedures. *Fac*-[Re(CO)$_3$(phen)Br],[24] *fac*-[Re(CO)$_3$(bipy)(MeCN)]BF$_4$, and *fac*-[Re(CO)$_3$(phen)(MeCN)]BF$_4$[25] were prepared according to the literature procedures. Nicotinoyl chloride was prepared by simply stirring and heating nicotinic acid in $SOCl_2$ until complete dissolution was evident; the solvent was then removed in vacuo, and the crude product (nicotinoyl chloride) used immediately, without further purification. **L5** and **L6**[26] were prepared according to the literature methods. All other starting materials were used as purchased.

Synthesis of L1. Laurinlactam (13 g, 0.065 mols) was dissolved in 6 M HCl (150 mL) and heated at 150 °C for 24 h. The green solution was allowed to cool and the resultant precipitate was filtered giving 12-aminolauric acid as the hydrogen chloride salt (Yield: 10.2 g, 73%). ^{1}H NMR (CD_3OD, 400 MHz, 298 K) δ_H: 2.83 (2H, t, $^{3}J_{HH}$ = 7.6 Hz), 2.30 (2H, t, $^{3}J_{HH}$ = 7.4 Hz), 1.66−1.53 (4H, m), 1.38−1.15 (14H, s) ppm. MS (ES$^+$) m/z: 216.2 [M+H]$^+$. 12-Aminolauric acid hydrogen chloride (1.00 g, 3.98 mmol) and phthalic anhydride (0.589 mg, 3.98 mmol) were subsequently added to a Schlenk tube and heated until evolution of water vapor ceased giving a brown solid. ^{1}H NMR (CD_3OD, 400 MHz, 298 K) δ_H: 7.70−7.82 (4H, m), 3.63 (2H, t, $^{3}J_{HH}$ = 6.3 Hz), 3.28−3.23 (2H, m), 2.23 (2H, t, $^{3}J_{HH}$ = 6.8 Hz), 1.62−1.50 (4H, m), 1.37−1.13 (12H, m) ppm.

This crude product (1.3 g, 3.72 mmol) was then dissolved in thionyl chloride (2 mL) and left at 71 °C for 1 h. The excess thionyl chloride was removed under reduced pressure and to this was added chloroform (20 mL), triethylamine (1.14 mL, 11.14 mmol), and 3-aminomethyl pyridine (0.76 mL, 7.43 mmol) and the mixture heated to 59 °C for 3 h. Solvents were removed under vacuum and the product was washed using sat. aq. ammonium chloride (3 × 10 mL). The organic layer was dried and solution evaporated to give **L1** (Yield: 1.48 g, 95%). ^{1}H NMR ($CDCl_3$, 400 MHz, 298 K) δ_H: 8.51−8.44 (2H, m), 7.80−7.72 (2H, m), 7.69−7.61 (2H, m), 7.55−7.52 (1H, m), 7.20−7.17 (1H, m), 6.47 (1H, s, N*H*), 4.32 (2H, d, $^{3}J_{HH}$ = 4.3 Hz), 3.58 (2H, t, $^{3}J_{HH}$ = 7.5 Hz), 2.19 (2H, t, $^{3}J_{HH}$ = 7.3 Hz), 1.66−1.39 (4H, m), 1.29−1.01 (14H, m) ppm. ^{13}C{^{1}H} NMR ($CDCl_3$, 101 MHz, 298 K) δ_C: 173.3, 168.5, 149, 148.7, 135.6, 134.2, 133.9, 132.2, 123.5, 123.1, 40.9, 38.1, 36.7, 29.4, 29.4, 29.2, 29.1, 28.6, 26.8, 25.7 ppm. MS (ES$^+$) m/z: 435.33 [M+H]$^+$. HRMS (ES$^+$) found m/z 436.2588 [M+H]$^+$; [$C_{26}H_{33}O_3N_3$]$^+$ requires 436.2595. UV−vis. (ε/M^{-1} cm^{-1}) (MeCN) λ_{max}: 259 (14700), 294 (6400) nm. IR (nujol) υ: 1772 (CO), 1715 (CO) cm^{-1}.

Synthesis of L2. **L1** (1.2 g, 2.84 mmol) was dissolved in methoxyethanol (20 mL), hydrazine (0.41 mL, 0.854 mmol) added, and the solution stirred at 115 °C for 12 h. The solution was then allowed to cool, the white precipitate removed by filtration, and the filtrate evaporated to dryness. The filtrate was then stirred in hot chloroform and refiltered. The solvent was removed by evaporation, producing a creamy white solid as precursor **pro-L2** (Yield: 0.5 g, 58%). ^{1}H NMR ($CDCl_3$, 400 MHz, 298 K) δ_H: 8.46−8.38 (2H, m), 7.53 (1H, d, $^{3}J_{HH}$ = 7.5 Hz), 7.12−7.05 (1H, m), 4.44 (2H, d, $^{3}J_{NH}$ = 5 Hz), 2.55 (2H, t, $^{3}J_{HH}$ = 12.5 Hz), 1.63 (2H, t, $^{3}J_{HH}$ = 7.5 Hz), 1.59 (2H, t, $^{3}J_{HH}$ = 6.2 Hz), 1.27−1.10 (16H, m) ppm. ^{13}C{^{1}H} NMR ($CDCl_3$, 101 MHz, 298 K) δ_C: 148.1, 147.7, 134.6, 122,6, 41.1, 39.9, 35.6, 33.5, 32.5, 28.5, 28.5, 28.4, 28.3, 28.2, 25.8, 24.7, 24.5 ppm. MS (ES$^+$) m/z: 306.3 [M+H]$^+$. HRMS (ES$^+$) found m/z 306.2537 [M+H]$^+$; [$C_{18}H_{32}ON_3$]$^+$ requires 306.2540.

This product (0.1 g, 0.38 mmol) was added to nicotinoyl chloride (0.055 g, 0.39 mmol), chloroform (20 mL), triethylamine (0.14 mL, 0.93 mmol), and the mixture heated to 59 °C for 3 h. Solvents were removed under vacuum, and the product was washed using sat. aq. ammonium chloride (3 × 10 mL). The organic layer was dried ($MgSO_4$), and solvent removed to give **L2** (Yield: 0.125 g, 93%). ^{1}H NMR ($CDCl_3$, 400 MHz, 298 K) δ_H: 8.91−8.88 (1H, m), 8.56−8.51 (1H, m), 8.48−8.39 (2H, m), 8.00 (1H, d), 7.50 (1H, d, $^{3}J_{HH}$ = 7.8 Hz), 7.34−7.25 (1H, m), 7.20−7.13 (1H, m), 6.48 (1H, s, N*H*), 6.1 (1H, s, N*H*), 4.45 (2H, d, $^{3}J_{HH}$ = 5.9 Hz), 3.38 (2H, m), 2.15 (2H, t, $^{3}J_{HH}$ = 7.6 Hz), 1.71−1.48 (4H, m), 1.35−1.02 (14H, m) ppm. ^{13}C{^{1}H} NMR ($CDCl_3$, 101 MHz, 298 K) δ_C: 156.8, 149.1, 148.8, 147.8, 135.9, 135.3, 123.7, 123.6, 65.2, 49, 40.1, 36.7, 29.5, 29.3, 29.2, 26.9, 25.7 ppm. MS (ES$^+$) m/z: 411.3 [M+H]$^+$, 433.3 [M+Na]$^+$. HRMS (ES$^+$) found m/z 411.2749 [M+H]$^+$; [$C_{24}H_{35}O_2N_4$]$^+$ requires 411.2755. UV−vis (ε/M^{-1} cm^{-1}) (MeCN) λ_{max}: 260 (9900) nm. IR (nujol) υ:1633 (CO) cm^{-1}.

Synthesis of L3. Nicotinoyl chloride (1.77 g, 12.48 mmol) in chloroform was added slowly to a solution of 1,12-dodecanediol (1.0 g, 4.99 mmol) and triethylamine (2.1 mL, 14.97 mmol) in chloroform (40 mL). The solution was left to stir at 60 °C for 5 h. The solution was washed with water (3 × 10 mL) and sat. aq. ammonium chloride (10 mL). The organic layer was dried and the solvent evaporated to dryness, yielding a white solid (Yield: 1.90 g, 93%). ^{1}H NMR ($CDCl_3$, 400 MHz, 298 K) δ_H: 9.12 (2H, s), 8.72−8.68 (2H, m), 8.27−8.21 (2H, m), 7.36−7.30 (2H, m), 4.75 (4H, t, $^{3}J_{HH}$ = 6.7 Hz), 1.79−1.69 (4H, m), 1.48−1.43 (4H, m), 1.32−1.13 (12H, m) ppm. ^{13}C{^{1}H} NMR ($CDCl_3$, 101 MHz, 298 K) δ_C: 164.2, 152.1, 149.7, 136.2, 125.4, 122.3, 64.6, 28.9, 28.5, 28.2, 27.6, 24.9 ppm. MS (ES$^+$) m/z: 413.2 [M+H]$^+$.

Synthesis of L4. **Pro-L2** (0.200 g, 0.655 mmol) and benzol-1,-2,4,5-benzenetetracarboxylicdianhydride (0.071 g, 0.323 mmol) were heated together in a Schlenk tube until the evolution of water vapor ceased, producing a brown solid (Yield: 0.251 g, 98%). ^{1}H NMR ($CDCl_3$, 250 MHz, 298 K) δ_H: 8.49 (4H, m), 8.22 (2H, d), 7.57 (2H, d, $^{3}J_{HH}$ = 7.5 Hz), 7.21−7.18 (2H, m), 4.41 (4H, d, $^{3}J_{HH}$ = 6.3 Hz), 3.17 (4H, t, $^{3}J_{HH}$ = 1.5 Hz), 2.18 (4H, t, $^{3}J_{HH}$ = 15 Hz), 1.64−1.60 (8H, m), 1.41−1.32 (28H, m) ppm. ^{13}C{^{1}H} NMR ($CDCl_3$, 101 MHz, 298 K) δ_C: 172.3, 165.3, 165.1, 164.7, 149, 148.5, 147.8, 147.5, 136.4, 136.2, 135.9, 135.8, 134.9, 133.4, 122.8, 122.7, 117.4, 117.1,

dx.doi.org/10.1021/ic201654d | Inorg. Chem. 2012, 51, 1419−1426

39.9, 38.7, 37.7, 35.6, 28.4, 28.3, 28.2, 28, 27.4, 25.7, 24.7 ppm. MS (ES^+) m/z: 793.5 $[M+H]^+$, 815.5 $[M+Na]^+$. HRMS (ES^+) found m/z 793.4634 $[M+H]^+$; $[C_{46}H_{61}O_6N_6]^+$ requires 793.4647. UV–vis (ε/M^{-1} cm^{-1}) (MeCN) λ_{max}: 274 (16100), 372 sh (7000) nm. IR (nujol) υ: 1740 (CO), 1696 (CO) cm^{-1}.

Synthesis of *fac*-[Re(CO)$_3$(1,10-phenanthroline)(L1)]BF$_4$ (Re-phen-L1). To a round-bottom flask encased in aluminum foil, $AgBF_4$ (31 mg, 0.14 mmol), $[ReBr(CO)_3(phen)]$ (57 mg, 0.1 mmol), **L1** (50 mg, 0.12 mmol) and toluene (10 mL) were added and heated to 100 °C for 12 h. The solution was filtered through Celite and washed repeatedly with acetonitrile until the solution ran clear. The removal of the solvent under high vacuum afforded a yellow solid. The crude product was purified using column chromatography eluting with dichloromethane:methanol (98:2) and reprecipated from chloroform and excess diethyl ether. (Yield: 27 mg, 28%). ^1H NMR ($CDCl_3$, 400 MHz, 298 K) δ_H: 9.52–9.49 (2H, m), 8.69–8.63 (2H, m), 8.17–8.10 (2H, m), 8.09–8.04 (1H, m), 8.0 (2H, s), 7.73–7.70 (3H, m), 7.62–7.58 (4H, m), 7.69–7.03 (1H, m), 4.19 (2H, t, $^3J_{HH}$ = 6 Hz), 3.59 (2H, t, $^3J_{HH}$ = 7.3 Hz), 1.96 (2H, t, $^3J_{HH}$ = 7.7 Hz), 1.64–1.60 (2H, m), 1.41–1.32 (2H, m), 1.20–1.11 (14H, m) ppm. $^{13}C\{^1H\}$ NMR ($CDCl_3$, 101 MHz, 298 K) δ_C: 174.6, 168.9, 154.6, 152.0, 150.0, 146.8, 140.5, 140.5, 139.9, 135.1, 134.3, 132.5, 131.8, 131.5, 128.8, 128.1, 126.5, 124.1, 123.6, 53.9, 40.6, 38.5, 36.4, 34.5, 29.9, 29.8, 29.7, 29.6, 27.3, 26.1, 25.9, 22.8 ppm. MS (ES^+) m/z: 886.3 $[M+H\text{-}BF_4]^+$. HRMS (ES^+) found m/z 884.2570; $[^{185}ReC_{41}H_{41}O_6N_5]^+$ requires 884.2581. IR (nujol) υ: 2032 (CO), 1921 (CO), 1711 (CO amide) cm^{-1}. UV–vis (ε/M^{-1} cm^{-1}) (MeCN) λ_{max}: 275 (29600), 365 (3400) nm. Anal. calcd (%) for $BC_{41}F_4H_{41}N_5O_6Re{\cdot}CHCl_3$: C, 48.93; H, 4.79; N, 5.94. Found (%): C, 48.93; H, 4.65; N, 6.08.

Synthesis of *fac*-{[Re(CO)$_3$(1,10-phenanthroline)]$_2$(L2)}(BF$_4$)$_2$ (Re2-phen-L2). To a round-bottom flask encased in aluminum foil, $AgBF_4$ (40 mg, 0.2 mmol), $[ReBr(CO)_3(phen)]$ (70 mg, 0.13 mmol), **L2** (27 mg, 0.06 mmol), and toluene (10 mL) were added and heated to 100 °C for 12 h. The solution was filtered over Celite and washed repeatedly with acetonitrile until the solution ran clear. The removal of the solvent under high vacuum afforded a yellow solid. The crude product was purified using column chromatography and eluting with dichloromethane:methanol (96:4). (Yield: 21 mg, 24%). ^1H NMR ($CDCl_3$, 400 MHz, 298 K) δ_H: 9.53–9.49 (5H, m), 8.78–8.71 (5H, m), 8.49–8.44 (1H, m), 8.25 (1H, m), 8.03–7.61 (8H, m), 7.62–7.58 (1H, m), 7.52 (1H, d), 7.20–7.15 (1H, m), 7.06–7.04 (1H, m), 6.92 (1H, s, N*H*), 6.61 (1H, s, N*H*), 4.31 (2H, d), 3.95–3.90 (2H, m), 1.55–1.52 (2H, m), 1.40–1.36 (2H, m), 1.29–1.11 (16H, m) ppm. MS (ES^+) m/z: 861.29 $[M\text{-}Re(CO)_3(phen)]$, 655.66 $[M+H]^{2+}$. HRMS (ES^+) found m/z 859.2737; $[^{185}ReC_{39}H_{42}O_5N_6]^+$ requires 859.2741. IR (nujol) υ: 2031 (CO), 1910 (CO), 1675 (CO amide) cm^{-1}. UV–vis (ε/M^{-1} cm^{-1}) (MeCN) λ_{max}: 252 (15760), 272 (15520), 342 (5100) nm. Anal. calcd (%) for $B_2C_{54}F_8H_{50}N_8O_8Re_2{\cdot}3CH_2Cl_2$ C, 39.35; H, 3.24; N, 6.44. Found (%): C, 39.24; H, 3.60; N, 6.69.

Synthesis of *fac*-{[Re(CO)$_3$(1,10-phenanthroline)]$_2$(L3)}(BF$_4$)$_2$ (Re2-phen-L3). To a round-bottom flask encased in aluminum foil, $AgBF_4$ (8.5 mg, 4.4×10^{-5} mol), $[ReBr(CO)_3(phen)]$ (30 mg, 7.39×10^{-5} mol), **L3** (14 mg, 3.69×10^{-5} mol) and toluene (10 mL) were added and heated to 100 °C for 12 h. The solution was filtered through Celite and washed repeatedly with acetonitrile until the solution ran clear. The filtrate was evaporated, and a yellow solid recrystallized from dichloromethane and diethyl ether (Yield: 19 mg, 26%). ^1H NMR (CD_3CN, 400 MHz, 298 K) δ_H: 9.54–9.51 (4H, m), 8.72 (4H, d), 8.48 (2H, s), 8.31 (2H, d), 8.06–8.02 (6H, m), 7.99–7.97 (4H, m), 7.42–7.23 (2H, m), 4.04 (4H, t, $^3J_{HH}$ = 6.6 Hz), 2.05–1.92 (4H, m), 1.58–1.50 (4H, m), 1.31–1.13 (12H, m) ppm. $^{13}C\{^1H\}$ NMR ($CDCl_3$, 101 MHz, 298 K) δ_C: 162.9, 155.6, 154.6, 152.0, 146.7, 140.6, 140.4, 131.5, 129.2, 128.3, 127.2, 126.7, 66.0, 29.9, 29.4, 28.1 ppm. MS (ES^+) m/z: 863.3 $[M\text{-}(Re(CO)_3(Phen)+H]^+$. HRMS ($ES^+$) found m/z 861.2404; $[^{185}ReC_{39}H_{40}O_7N_4]^+$ requires 861.2421. IR (nujol cm^{-1}) υ: 2034 (CO), 1917 (CO), 1722 (CO ester) cm^{-1}. UV–vis (ε/M^{-1} cm^{-1}) (MeCN) λ_{max}: 252 (24400), 275 (26600), 377 (2900) nm. Anal. calcd (%) for $B_2C_{54}F_8H_{48}N_6O_{10}Re_2{\cdot}0.75CH_2Cl_2$: C, 42.40; H, 3.22; N, 5.42. Found (%): C, 42.13; H, 3.87; N, 5.80.

Synthesis of *fac*-{[Re(CO)$_3$(1,10-phenanthroline)]$_2$(L4)}(BF$_4$)$_2$ (Re2-phen-L4). To a round-bottom flask was added, $[Re(CO)_3(phen)(MeCN)]BF_4$ (50 mg, 0.1 mmol), **L4** (40 mg, 0.05 mmol) and chloroform (10 mL) and heated to 59 °C for 12 h. The removal of the solvent under high vacuum afforded an orange colored solid. The crude product was purified using column chromatography, eluting with dichloromethane:methanol (96:4) (Yield: 16 mg, 14%). ^1H NMR ($CDCl_3$, 400 MHz, 298 K) δ_H: 9.49 (4H, m), 8.72 (4H, d), 8.1 (2H, s), 8.0 (12H, m), 7.49 (2H, d, $^3J_{HH}$ = 7.9 Hz), 7.05–7.00 (2H, m), 6.62 (2H, s, N*H*), 3.93 (4H, d, $^3J_{HH}$ = 6 Hz), 3.57 (4H, t, $^3J_{HH}$ = 7.2 Hz), 1.65 (4H, t, $^3J_{HH}$ = 6.7 Hz), 1.37 (4H, t, $^3J_{HH}$ = 7.0 Hz), 0.98–1.13 (32H, m) ppm. MS (ES^+) m/z: 846.2 $[M+H]^{2+}$, 1243.5 $[M\text{-}(Re(CO)_3Phen)]^+$, 1779.5 $[M\text{-}BF_4]^+$. HRMS (ES^+) found m/z 845.2373; $[^{185}Re_2C_{76}H_{76}O_{12}N_{10}]^{2+}$ requires 845.2346. IR (nujol) υ: 2032 (CO), 1917 (CO), 1717 (CO amide) cm^{-1}. UV–vis (ε/M^{-1} cm^{-1}) (MeCN) λ_{max}: 274 (17500) nm, 375 (5100) nm. Anal. calcd (%) for the corresponding hexafluorophosphate salt, $C_{76}F_{12}H_{76}N_{10}O_{12}P_2Re_2{\cdot}1.5CH_2Cl_2$: C, 44.08; H, 3.78; N, 6.64. Found (%): C, 44.06; H, 3.80; N, 6.38.

Synthesis of *fac*-{[Re(CO)$_3$(2,2′-bipyridine)]$_2$(L5)}(BF$_4$)$_2$ (Re2-bipy-L5). The complex was prepared by the addition of **L5** (hexyl dinicotinamide; 0.050 g, 15 mmol) to $[Re(CO)_3(bipy)(MeCN)]BF_4$ (0.159 g, 31 mmol) in ethanol (10 mL). The solution was heated to just below reflux with stirring overnight. The product precipitated as the solution was cooled and the yellow solid was filtered under vacuum and washed. Subsequent reprecipation from dichloromethane with diethyl ether gave the pure yellow solid (Yield: 0.136 g, 69%). ^1H NMR (CD_3CN, 400 MHz, 298 K) δ_H: 9.15 (4H, d, $^3J_{HH}$ = 5.2 Hz), 8.46 (2H, s), 8.32 (4H, d, $^3J_{HH}$ = 8.0 Hz), 8.25 (2H, d, $^3J_{HH}$ =5.6 Hz), 8.21–8.18 (4H, m), 8.07 (2H, d, $^3J_{HH}$ = 6.8 Hz), 7.73–7.69 (4H, m), 7.17 (2H, bs), 3.21–3.16 (4H, m), 1.46–1.38 (4H, m), 1.23–1.18 (4H, bm) ppm. $^{13}C\{^1H\}$ (CD_3CN, 62.5 MHz, 298 K) δ_C: 195.2 (CO), 162.3, 155.5, 153.5, 150.8, 140.9, 137.4, 132.8, 128.5, 125.7, 124.5, 39.9, 28.5, 26.2 ppm. MS (ES^+) m/z: 1265.2 $[M\text{-}BF_4]^+$. HRMS (ES^+) found m/z 1262.1902; $[^{185}Re_2C_{44}H_{38}O_8N_8{}^{10}BF_4]^+$ requires 1262.1938. IR (CH_3CN) ν: 2036 (CO), 1933 (CO), 1672 (CO amide) cm^{-1}. UV–vis (ε/M^{-1} cm^{-1}) (MeCN) λ_{max}: 305 (15000), 319 (14900) 333 (5400) nm. Anal. calcd (%) for $B_2C_{44}F_8H_{38}N_8O_8Re_2{\cdot}0.75CH_2Cl_2$: C, 37.93; H, 2.82; N, 7.91. Found (%): C, 38.12; H, 2.45; N, 8.23.

Synthesis of *fac*-{[Re(CO)$_3$(2,2′-bipyridine)]$_2$(L6)}(BF$_4$)$_2$ (Re2-bipy-L6). The complex was prepared by the addition of **L6** (octyl dinicotinamide; 0.050 g, 14 mmol) to $[Re(CO)_3(bipy)(MeCN)]BF_4$ (0.146 g, 28 mmol) in ethanol (10 mL). The solution was heated to subreflux with stirring overnight. The product was reprecipated from dichloromethane and diethyl ether and then filtered under vacuum to give a yellow solid (Yield: 0.094 g, 51%). ^1H NMR (CD_3CN, 250 MHz, 298 K) δ_H: 9.17 (4H, d, $^3J_{HH}$ = 0.8 Hz), 8.45 (2H, d, $^3J_{HH}$ =1.6 Hz), 8.31 (4H, d, $^3J_{HH}$ = 8.4 Hz), 8.25 (2H, d, $^3J_{HH}$ = 5.2 Hz), 8.19 (4H, dd, J = 8.4 and 1.6 Hz), 8.05 (2H, dt, J = 1.6, 8.0 Hz), 7.73–7.68 (4H, m), 7.29 (2H, m), 7.09 (2H, bs), 3.21–3.16 (4H, m), 1.46–1.39 (4H, m), 1.24–1.17 (8H, m) ppm. $^{13}C\{^1H\}$ (CD_3CN, 62.5 MHz, 298 K) δ_C: 195.3 (CO), 162.7, 155.5, 153.4, 150.8, 140.9, 137.4, 132.9, 128.5, 126.0, 124.5, 40.9, 39.0, 28.5, 25.5 ppm. HRMS (ES^+) found m/z 1290.2291; $[^{185}Re_2C_{46}H_{42}O_8N_8{}^{10}BF_4]^+$ requires 1290.2251. IR (CH_3CN) ν: 2036 (CO), 1933 (CO), 1635 (CO amide) cm^{-1}. UV–vis (ε/M^{-1} cm^{-1}) (MeCN) λ_{max}: 308 (26200), 319 (26100), 336 (8900) nm. Anal. calcd (%) for $B_2C_{46}F_8H_{42}N_8O_8Re_2{\cdot}H_2O{\cdot}CH_2Cl_2$: C, 38.05; H, 2.99; N, 7.55. Found (%): C, 38.29; H, 2.52; N, 7.78.

RESULTS AND DISCUSSION

Synthesis of the Ligands and Complexes. Each of the ligands was synthesized from commercially available pyridine-type starting materials (nicotinic acid or 3-aminomethyl pyridine). **L1** was isolated by preparing the phthalimido precursor, through acid-promoted ring-opening hydrolysis of laurinlactam to give 12-aminolauric acid; subsequent reaction with phthalic anhydride gave the corresponding phthalimide precursor. This synthon was converted to the corresponding acid

dx.doi.org/10.1021/ic201654d | Inorg. Chem. 2012, 51, 1419–1426

chloride and then reacted with 3-aminomethyl pyridine to give **L1**. Deprotection of **L1** produced the corresponding free amine, **pro-L2** (Scheme 1), where **L2** then required further addition of

Scheme 1. Synthesis of Selected Ligands[a]

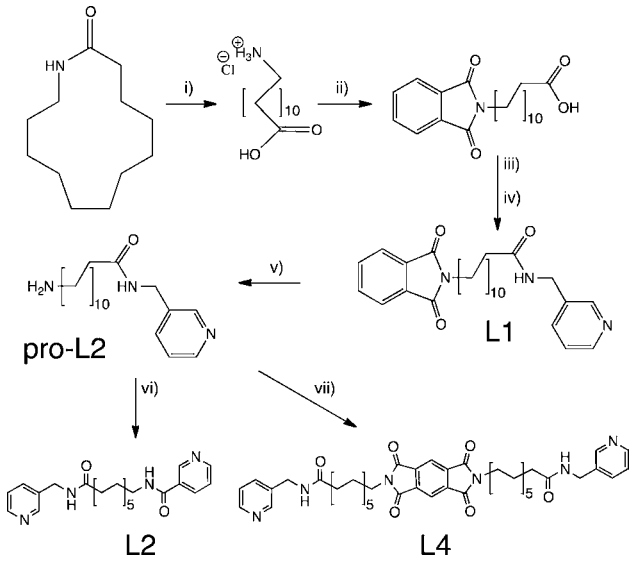

[a]Reagents: (i) 6 M HCl; (ii) phthalic anhydride, Δ; (iii) $SOCl_2$; (iv) 3-aminomethylpyridine; (v) hydrazine hydrate, Δ; (vi) nicotinoyl chloride; (vii) pyromellitic dianhydride, Δ.

nicotinoyl chloride. Reaction of **pro-L2** with 0.5 equiv of benzol-1,2,4,5-benzenetetracarboxylicdianhydride (pyromellitic dianhydride) gave **L4**, wherein a pyromellitic-diimide (PMDI) chromophore is incorporated into the alkyl chain framework. **L3** was simply isolated following reaction of 1,12-dodecanediol with excess nicotinoyl chloride. Similarly, **L5** (via 1,6-diaminohexane) and **L6** (via 1,8-diaminooctane) were prepared through coupling of the appropriate diamines with excess nicotinoyl chloride.[10] Each of the new ligands were fully characterized using comprehensive spectroscopic analyses and mass spectrometry. The syntheses of the cationic rhenium complexes (Scheme 2) were achieved following literature precedent, using either *fac*-[$Re(CO)_3$(bipy)(MeCN)](BF_4) or *fac*-[$Re(CO)_3$(phen)(Br)] as required;[2,27] the pure mono- and dimetallic complexes were isolated either as their tetrafluoroborate or hexafluorophosphate salts. Spectroscopic characterization of the complexes was achieved using ^1H and $^{13}C\{^1H\}$ NMR, IR and UV−vis. spectroscopies. Additional analytical data was provided through elemental analyses and mass spectrometry, which was obtained on the complexes and frequently revealed peaks at m/z observed for the dicationic species ($z = 2$), as well as fragmentation of the axial ligands resulting in the loss of one "$Re(CO)_3$(phen)" unit.

Luminescence Properties of the Ligands and Complexes. The absorption properties of the complexes are characterized by two common features: ligand-centered (diimine, pyridine, or phthalimido) and metal-to-ligand charge transfer transitions (^{1}MLCT). The former typically predominate <320 nm, whereas the latter contribute to the pale yellow colored appearance of the complexes (>320 nm).[24,25] In the case of **L4** there are additional contributions from the PMDI chromophore between 300 and 350 nm.

In aerated MeCN solution at room temperature, the emission properties of **L1** and **L4** show a longest wavelength emission (ca. 400−410 nm), which was characterized as a

Scheme 2. Rhenium Complexes Synthesized in This Study

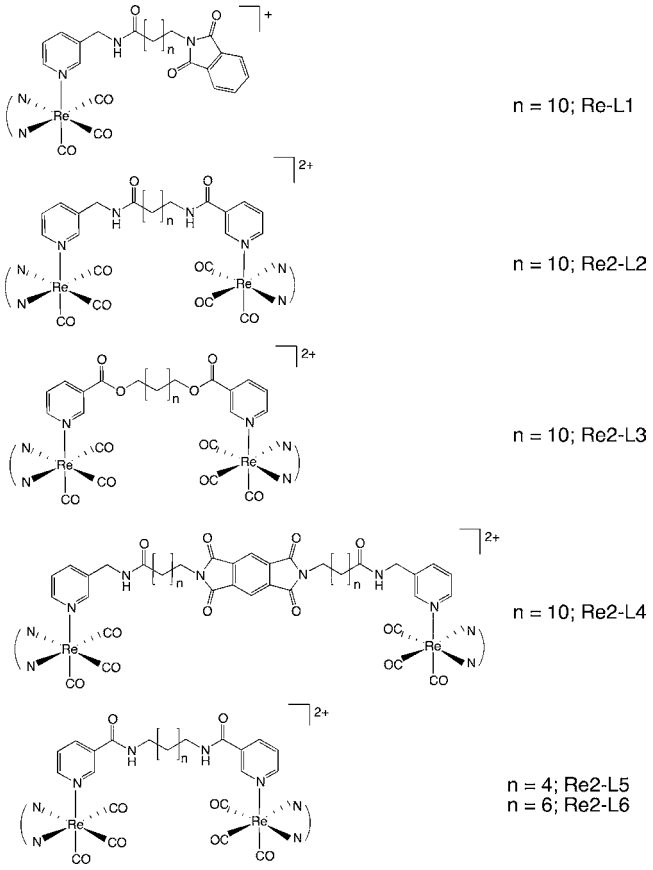

short-lived fluorescence, and attributed to the $^1\pi-\pi^*$ state of the chromophores in each case. The emission from **L4** is therefore characteristic of a monomeric PMDI, rather than excimer-type, fluorescent state. For **L1** these observations are consistent with our previous work on phthalimide-appended pyridyl-type ligands.

For the complexes, sensitization of the ^{1}MLCT at around 380 nm resulted in characteristic long-lived ^{3}MLCT emission at around 540 nm (phenanthroline derivatives) or 560 nm (bipyridine derivatives), with corresponding quantum yields in the 3.2−8.0% range.[24,25] In aerated MeCN the emission profiles were typically broad and featureless in appearance, and the lifetimes were satisfactorily fitted to single exponential decays in each case, suggesting that for the dimeric species both rhenium diimine chelates are in the same excited state environment. As reported for closely related systems,[28,29] the lifetime of the phenanthroline complexes are typically much longer than related bipyridine analogues, reflecting both the enhanced rigidity and the higher energy emission wavelength of the former.

For **Re2-phen-L4**, the overlapping absorption bands of the ^{1}MLCT and bridging PMDI-type chromophore infer that both chromophoric units can be sensitized (λ_{ex} = 345 nm), revealing a complex that is dual-emissive: a higher energy (i.e., monomer-type) band at about 405 nm[30] attributed to the PMDI fluorophore that is relatively unperturbed compared to the free ligand (cf. 420 nm) and second, a broad, lower energy band (541 nm) assigned to the ^{3}MLCT emitting state. The fluorescence lifetime of the PMDI-based emission is shorter than for the free ligand (2.6 vs 4.9 ns) suggesting some degree of quenching in the presence of the rhenium units. In contrast to the other complexes, the decay profile for the ^{3}MLCT band

dx.doi.org/10.1021/ic201654d | Inorg. Chem. 2012, 51, 1419−1426

Table 1. UV-visible Absorption and Emission Data for the Complexes

compound	λ_{abs} (^{1}MLCT)/nm[a]	λ_{em}/nm[a]	$\Phi^{a,b}$	τ_{3MLCT}/ns[a]	λ_{em}/nm[c]	τ_{3MLCT}/ns[c]
$[Re(CO)_3phen(L1)]BF_4$	365	546	0.080	248	543	338
$\{[Re(CO)_3phen]_2L2\}(BF_4)_2$	342	547	0.048	215	540	510
$\{[Re(CO)_3phen]_2L3\}(BF_4)_2$	377	541	0.064	248	546	444
$\{[Re(CO)_3phen]_2L4\}(BF_4)_2$	365	405,541	0.050	46, 202	421, 537	27, 332
$\{[Re(CO)_3bipy]_2L5\}(BF_4)_2$	333	551	0.050	136	555	132
$\{[Re(CO)_3bipy]_2L6\}(BF_4)_2$	336	553	0.032	129	550	149

[a]In aerated acetonitrile. [b]Quantum yields obtained using a reference value of 0.016 for $[Ru(bpy)_3](PF_6)_2$ in aerated acetontrile. [c]In aerated water. Steady state spectra obtained using λ_{ex} = 345 nm. Lifetimes obtained using λ_{ex} = 372 nm (errors ±10%).

could not be fitted to a single-exponential component, but rather, a biexponential decay provided a better fit for the data (as judged by the summed residual squared errors of the associated fit), giving two distinct lifetimes of 202 (~75% of the total decay intensity) and 46 ns (Table 1). The former lifetime is clearly comparable in magnitude to $\tau_{(MLCT)}$ of the complexes of **L1**-**L3**, whereas the latter component is shorter than expected for unperturbed ^{3}MLCT emission originating from the cationic complex core (*cf.* **Re-phen-L1**); the quantum yield of **Re2-phen-L4** is also lower than the structurally related complex **Re-phen-L1**. With comparison to the other emissive complexes in this series, prospective quenching pathways for the ^{3}MLCT state may involve the bridging PMDI-type chromophore. A commonly observed quenching pathway for ^{3} M_{Re}LCT excited states involves forward electron transfer from an available donor, generating a LLCT transient excited state (back electron transfer regenerates the ground MLCT state).[31] However, in this case the oxidation potential of PMDI (actually a very strong electron acceptor) should render such a process unfavorable from a thermodynamic perspective.[32] Alternatively, triplet−triplet energy transfer has been previously reported for related Re(I)-spacer-anthracene (i.e., chromophore-quencher) complexes where the observed ^{3}MLCT lifetimes were also shortened (mechanistically reported to proceed via Dexter electron exchange).[33,34] The energy transfer between ^{3}MLCT and ^{3}IL(anthracene) are much more favorable than those described here since, energetically, the triplet excited state of PMDI (19700 cm^{-1})[32] is above that of anthracene. In comparison the PMDI-centered $^3\pi-\pi^*$ state of **L4** (recorded at 77 K; 1:1, EtOH:MeOH glass) possessed vibronically structured peaks at 467 (21400 cm^{-1}) and 490 nm (20400 cm^{-1}), and these values suggest that there is some spectral overlap of the PMDI triplet state with the ^{3}MLCT emission profile, although triplet−triplet energy transfer does not appear to be particularly efficient (deaerated measurements did not result in an extension in the ^{3}MLCT lifetimes), as evidenced by the predominance of the longer lifetime value to the decay profile.

Luminescence measurements in aqueous media (<10^{-5} M) demonstrated that the majority of the complexes are sensitive to the nature of the solvent environment. Our previous studies have proposed the influence (and chain length dependence) of hydrophobically driven intramolecular interactions between long alkyl chains and the coordinated diimine unit, effectively resulting in shielding of the ^{3}MLCT excited state from the (quenching) solvent environment.[23] For the complexes of **L1**-**L4** the ^{3}MLCT emission was retained and moderately hypsochromically shifted, again consistent with shielding from the polar aqueous solvent. For these complexes the aqueous emission spectra also showed reversible temperature dependence within a narrow temperature range, wherein the emission intensity increased with decreasing temperature, together with a concomitant hypsochromic shift in λ_{em}; such dependence was not observed in MeCN over this temperature range. Although these trends are less pronounced than for the related monometallic complexes,[23] they are still consistent with an entropically driven chain-wrapping process which shields the ^{3}MLCT excited state from water solvent. For **Re2-phen-L4** the corresponding VT spectra (Figure 1) revealed the ratiometric

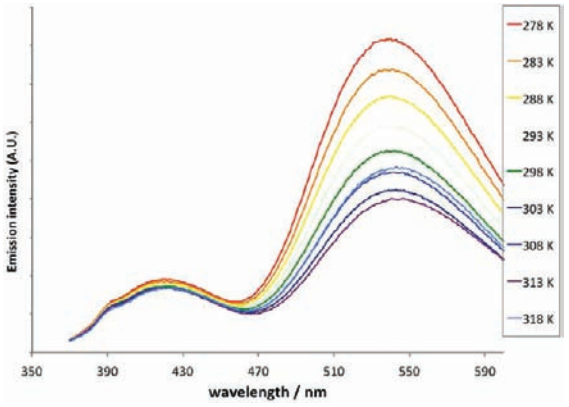

Figure 1. Steady state emission spectra for **Re2-phen-L4** recorded in water at temperatures between 278 and 318 K (excitation wavelength 345 nm).

responses of the dual-emission between 278 and 318 K, nicely demonstrating the relative sensitivities of the two different excited states ($^1\pi-\pi^*$ of PMDI at about 420 nm, and ^{3}MLCT at about 535 nm) to the polar solvent environment. Accordingly, the dipolar ^{3}MLCT excited state showed marked temperature dependence, consistent with solvation changes in the local environment.

The lifetimes were also extended in water, most noticeably for the nicotinamide derivative **Re2-phen-L2**, again suggesting that the excited state localized on the coordinated phenanthroline ligand was shielded from the quenching phenomena associated with water solvent. In contrast, for the shorter chain dimetallic species based on ligands **L5** and **L6**, the measurements in water did not show any significant deviations from those obtained in MeCN, suggesting that the alkyl chain length must exceed at least C8 to allow sufficient conformational freedom.[23]

Confocal Fluorescence Microscopy: Cellular Imaging. Having studied the photophysical properties of the dirhenium complexes, and established that they had suitable emission and excitation profiles for cell imaging applications, a series of live cell imaging experiments were undertaken. To assess the influence upon cell uptake and, in particular, intracellular localization of changing the chelating ligand and the nature and

dx.doi.org/10.1021/ic201654d | *Inorg. Chem.* 2012, 51, 1419−1426

length of the linker, the complexes were each incubated under the same conditions, and for the same period with MCF-7 cells. The incubations were carried out at 4 °C at which temperature energy-dependent uptake processes such as endocytosis are inhibited,[35] to avoid entrainment in endosomes, and to allow a comparison of the intrinsic membrane permeancy of the species. The cells were washed free of excess agent, then allowed to warm to ambient temperature to allow energy-dependent intracellular distribution pathways to re-emerge, while blocking energy-dependent uptake before examination by confocal laser microscopy. In all cases the excitation wavelength was 405 nm (at the low-energy edge of the ^{1}MLCT absorption band), and the images were collected between 530 and 580 nm, correlating to ^{3}MLCT emission, and well separated from autofluorescence.[6]

The reference monomeric species **Re-phen-L1** with a C11-linked phthalimide showed good uptake (Figure 2) with >80%

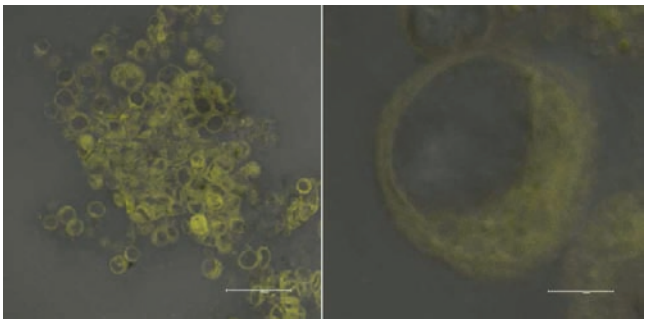

Figure 2. Uptake (left, scale bar = 48 μm) and localization (right, scale bar = 5 μm) of **Re-phen-L1** in MCF7s.

of the cell sample showing rhenium-based emission, consistent with the highly lipophilic structure, which will assist passive diffusion across membranes. Closer examination of individual cells (Figure 2) showed general staining, with plasma membrane, internal membranes, and the perinuclear region of the cytoplasm all showing strong emission with no evidence of nuclear uptake. No localized intense spots were observed in the cytoplasm, indicating nonspecific distribution throughout lipophilic structures, rather than specific uptake in particular organelles.

The dimeric, pyromellitate-linked species **Re2-phen-L4** also showed excellent uptake (Figure 3), with >80% of the cell

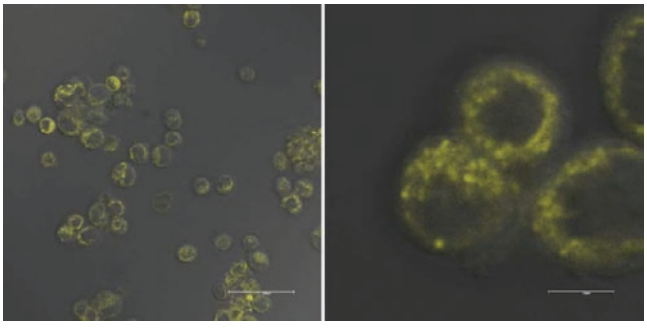

Figure 3. Uptake (left, scale bar = 48 μm) and localization (right, scale bar = 7 μm) of **Re2-phen-L4** in MCF7s.

sample showing rhenium-based emission, although the intensity was variable from cell to cell. There was a distinctive pattern to the cellular localization with some general background emission from membrane and cytoplasm, but with distinct bright spots, characteristic of organelle staining. It is likely that the organelles may include mitochondria, ER, and Golgi apparatus. The mitochondrial uptake is encouraged by the dicationic nature of the complex, enabling uptake across the mitochondrial membrane because of the significant membrane potential, maintained by the negative interior of the organelle with respect to the cytoplasm. However, the pattern of distribution is far too wide for specific mitochondrial uptake, in line with the requirement for rhenium complexes to be thiol-reactive to show specific mitochondrial staining,[23] while several lipophilic cationic examples have shown some, nonspecific mitochondrial uptake.[7]

Similarly, the nonsymmetrical dirhenium diamide **Re2-phen-L2** showed good uptake (Figure 4), with >80% of cells showing

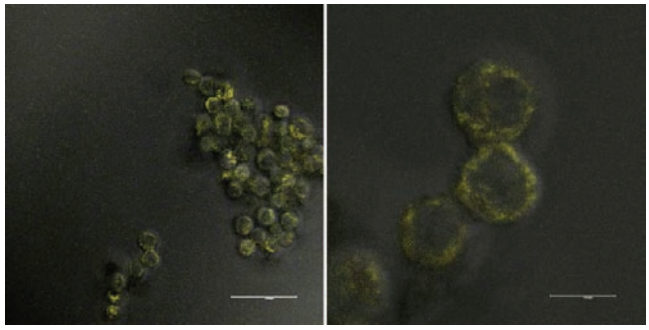

Figure 4. Uptake (left, scale bar = 48 μm) and localization (right, scale bar = 10 μm) of **Re2-phen-L2** in MCF7s.

rhenium based emission, but again there were wide variations in the intensity between cells. Again, localization in a large number of cytoplasmic structures giving a distinctive pattern of staining of the cytoplasmic organelles, but without evidence of specificity. This is consistent with the cationic and lipophilic nature of the complex, with no targeting vectors to direct specific localization to any given organelle.

The highly lipophilic diester species **Re2-phen-L3** showed excellent uptake with uniformly intense emission from >90% of the cell sample, with diffuse cytoplasmic and membrane staining, with brighter staining characteristic of better uptake than the amide analogues (Figure 5). This higher uptake is

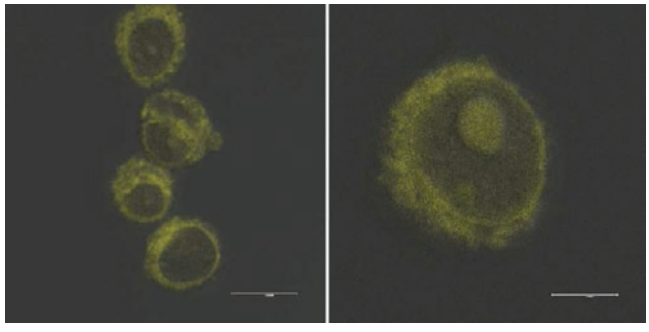

Figure 5. Uptake (left, scale bar = 14 μm) and nucleolar localization (right, scale bar = 10 μm) of **Re2-phen-L3** in MCF7s.

assigned to the lipophilicity associated with the aliphatic chain, combined with an absence of amide units, which have previously been noted[7] as showing lower uptake than esters in

dx.doi.org/10.1021/ic201654d | Inorg. Chem. 2012, 51, 1419–1426

pairs of analogous rhenium complexes. In addition to the excellent uptake observed with this complex, on a small number of occasions distinct bright spots of emission from the dark region of the cells correlating to the nucleus were observed, which is usually considered to be characteristic of nucleolar localization. As with the previous reports of highly lipophilic rhenium complexes which show nucleolar localization,[7] the small percentage of cells showing nuclear uptake (on the occasions that it was observed) made confirmation of nucleolar localization by colocalization experiments impossible. In the absence of colocalization, experiments were undertaken with the same cell line, under the same incubation conditions, with a known nucleolar stain, SYTORNASelect, (SRS) which is known to selectively stain the nucleoli of healthy mammalian cells (Figure 6). The patterns of staining of the nucleoli of the

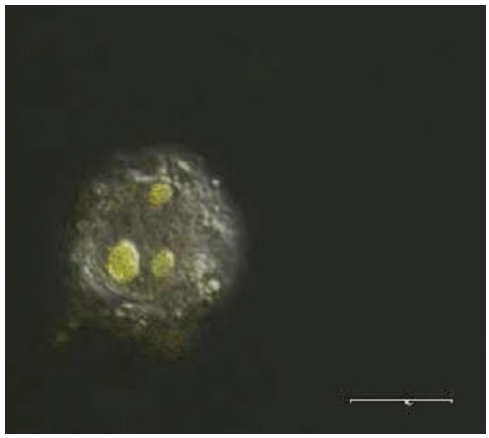

Figure 6. Localization of SRS (scale bar = 9 μm) in MCF7s.

cell samples with SRS were essentially identical to those observed with the diester, although the diester also showed cytoplasmic staining, providing strong support for the assignment of the staining as nucleolar. In addition, a series of Z-stacks[36] were collected confirming that the emission assigned as nucleolar came from within the central depth of the otherwise dark nuclear region of the cell, confirming that an intranuclear compartment had been stained, rather than a site on the cell surface. Even in the absence of colocalization data therefore, the confirmation that these bright spots represent staining of an intranuclear compartment, similar in size and shape to the nucleoli stained by SRS strongly indicates an assignment as nucleolar staining. This apparent nucleolar localization is assigned to the additional lipophilicity of ester species over amide analogues, allowing permeation of the nuclear membrane, and it is likely that the localization in the nucleolus is a result of Coulombic attraction between the dicationic complex and polyanionic poly- or oligo-nucleotides.

The pair of analogous diamide complexes, **Re2-bipy-L5** (L5 = 1,6-hexanedinicotinamide) and **Re2-bipy-L6** (L6 = 1,8-octanedinicotinamide) were also studied to assess the change in uptake upon replacing phenanthroline in the related complex **Re2-phen-L2** with bipyridine, and to compare the C8 and C6 analogues. Both **Re2-bipy-L5** and **Re2-bipy-L6** showed cellular uptake (Figure 7), but the level was much higher for the more lipophilic **Re2-bipy-L6** complex. The patterns of localization were similar with both agents showing accumulation in the cytoplasm, but the emission from cells stained with **Re2-bipy-L5** was more diffuse than

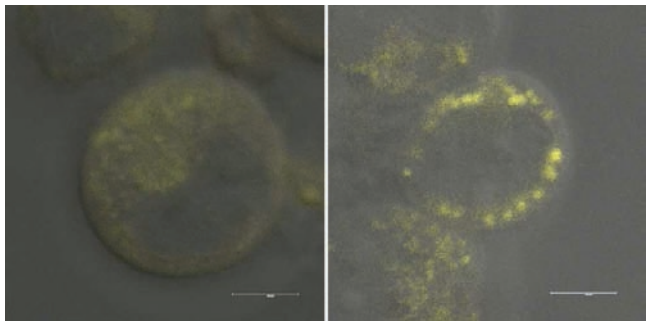

Figure 7. Localization of **Re2-bipy-L5** (left, scale bar = 6 μm) and **Re2-bipy-L6** (right, scale bar = 6 μm) in MCF7s.

that observed with **Re2-bipy-L6**, which showed clear accumulation in distinct organelles, as well as general background emission from the cytoplasm. This suggests that the greater lipophilicity of **Re2-bipy-L6** assists in permeating the internal membranes protecting organelles and allowsit to penetrate them and accumulate in the interior, rather than be associated with the exterior of the membranes.

Overall, it is clear that dimeric rhenium complexes, even those as large as **Re2-phen-L4** are taken up efficiently by MCF7s, by non-energy dependent mechanisms, without endosomal entrainment. The degree of uptake and the patterns of localization depend not only upon the length of the linker chain but also upon the nature of the linkages. Thus, the diester **Re2-phen-L3** is taken up best of all the complexes examined, even though on simple charge versus chain-length arguments monocationic **Re-phen-L1** might be expected to show best uptake. It has previously been noted[7] that the uptake of rhenium complexes is highly dependent upon small changes in structure which cannot be explained by simple lipophilicity arguments, and that in most cases esters are taken up better than the analogous amides. This phenomenon implies that even in the absence of endocytosis, specific interactions between the complex and the exterior of the cell membrane are important to uptake, making simple assumptions about permeancy–lipophilicity relationships unwise. Small changes in chain length (e.g., from **Re2-bipy-L5** to **Re2-bipy-L6**) can lead to noticeable changes in uptake and localization, reinforcing similar previous observations in related monomeric complexes. Finally, although no exactly analogous complexes were examined, the trends of uptake imply that 1,10-phenanthroline complexes are more effectively taken up than 2,2′-bipyridine derivatives, in line with the expected improvement in lipophilicity and the literature precedent for related ruthenium complexes.

The cytotoxicity of a small range of complexes was examined by the propidium iodide (PI) assay, in which cells are incubated first with the species of interest, then with PI, which only enters cells that have damaged membranes, itself an indicator of poor health. The complexes tested showed low cytotoxicity levels, with 1–7% of cells taking up PI, compared to 3% for a DMSO control, indicating that these are viable fluorophores for use in live cell imaging. The highest toxicity (7% PI stained cells) is associated with the highly lipophilic diester, **Re2-phen-L3**, in line with previous reports of highly lipophilic rhenium cations causing membrane disruption,[9] while the other complexes tested showed cytotoxicity below, or barely above, the blanks.

In summary, a series of luminescent dimetallic rhenium complexes linked through various chain lengths and functionalities have been synthesized and fully characterized. For chain lengths

dx.doi.org/10.1021/ic201654d | *Inorg. Chem.* 2012, 51, 1419–1426

greater than C8, the complexes show solvent-dependent photophysical properties consistent with hydrophobically driven intramolecular interactions in aqueous environments. The incorporation of a PMDI-type chromophore into the alkyl chain provides a complex that is dual emissive, with ratiometric sensitivity to solvent environment, wherein the PMDI unit appears to provide a potential quenching pathway for the ^{3}MLCT excited state. Each complex demonstrated great utility as an intracellular imaging probe for MCF7 cells, as evidenced through confocal fluorescence microscopy studies. The ester-linked dimetallic complex showed improved uptake over the related amide systems and specific organelle localization was promoted through the dicationic nature of the complexes.

AUTHOR INFORMATION

Corresponding Author

*E-mail: cooganmp@cardiff.ac.uk (M.P.C.), popesj@cardiff.ac.uk (S.J.A.P.).

ACKNOWLEDGMENTS

We thank Cardiff University and EPSRC for financial support and the staff of the EPSRC Mass Spectrometry National Service (University of Swansea) for providing MS data.

REFERENCES

(1) Lees, A. J. *Chem. Rev.* **1987**, *87*, 711−743.

(2) Sacksteder, L.; Zipp, A. P.; Brown, E. A.; Streich, J.; Demas, J. N.; DeGraff, B. A. *Inorg. Chem.* **1990**, *29*, 4335−4340.

(3) Worl, L. A.; Duessing, R.; Chen, P.; Della Ciana, L.; Meyer, T. J. *J. Chem. Soc., Dalton Trans.* **1991**, 849−858.

(4) Keefe, M. H.; Benkstein, K. D.; Hupp, J. T. *Coord. Chem. Rev.* **2000**, *205*, 201−228.

(5) Coleman, A.; Brennan, C.; Vos, J. G.; Pryce, M. T. *Coord. Chem. Rev.* **2008**, *252*, 2585−2595.

(6) Fernandez-Moreira, V.; Thorp-Greenwood, F. L.; Coogan, M. P. *Chem. Commun.* **2010**, *46*, 186−202.

(7) Fernandez-Moreira, V.; Thorp-Greenwood, F. L.; Amoroso, A. J.; Cable, J.; Court, J. B.; Gray, V.; Hayes, A. J.; Jenkins, R. L.; Kariuki, B. M.; Lloyd, D.; Millet, C. O.; Williams, C. F.; Coogan, M. P. *Org. Biomol. Chem.* **2010**, *8*, 3388−3901.

(8) Louie, M. W.; Lam, M. H. C.; Lo, K. K. W. *Eur. J. Inorg. Chem.* **2009**, 4265−4273.

(9) Amoroso, A. J.; Coogan, M. P.; Dunne, J. E.; Fernandez-Moreira, V.; Hess, J. B.; Hayes, A. J.; Lloyd, D.; Millet, C.; Pope, S. J. A.; Williams, C. *Chem. Commun.* **2007**, 3066−3068.

(10) Raszeja, L.; Maghnouj, A.; Hahn, S.; Metzler-Nolte, N. *ChemBioChem* **2011**, *12*, 371−376.

(11) Lo, K. K.-W.; Louie, M.-W.; Sze, K.-S.; Lau, J. S.-Y. *Inorg. Chem.* **2008**, *47*, 602.

(12) Ferri, E.; Donghi, D.; Panigati, M.; Prencipe, G.; D'Alfonso, L.; Zanoni, I.; Baldoli, C.; Maiorana, S.; D'Alfonso, G.; Licandro, E. *Chem. Commun.* **2010**, *46*, 6255−6257.

(13) Lo, K. K. W.; Louie, M. W.; Zhang, K. Y. *Coord. Chem. Rev.* **2010**, *254*, 2603−2622.

(14) Tan, W. J.; Zhou, J.; Li, F. Y.; Yi, T.; Tian, H. *Chem.—Asian J.* **2011**, *6*, 1263−1268.

(15) Xiong, L. Q.; Zhao, Q.; Chen, H. L.; Wu, Y. B.; Dong, Z. S.; Zhou, Z. G.; Li, F. Y. *Inorg. Chem.* **2010**, *49*, 6402−6408.

(16) Zhang, S. J.; Hosaka, M.; Yoshihara, T.; Negishi, K.; Iida, Y.; Tobita, S.; Takeuchi, T. *Cancer Res.* **2010**, *70*, 4490−4498.

(17) Jiang, W. L.; Gao, Y.; Sun, Y.; Ding, F.; Xu, Y.; Bian, Z. Q.; Li, F. Y.; Bian, J.; Huang, C. H. *Inorg. Chem.* **2010**, *49*, 3252−3260.

(18) Murphy, L.; Congreve, A.; Palsson, P. O.; Williams, J. A. G. *Chem. Commun.* **2010**, *46*, 8743−8745.

(19) Zhang, K. Y.; Lo, K. K. W. *Inorg. Chem.* **2009**, *48*, 6011−6025.

(20) See: Lakowicz, J.R. In *Principles of Fluorescence Spectroscopy*, 3rd ed.; Springer: New York, 2006, and references therein.

(21) Amoroso, A. J.; Arthur, R. J.; Coogan, M. P.; Court, J. B.; Fernandez-Moreira, V.; Hess, J. B.; Hayes, A. J.; Lloyd, D.; Millet, C.; Pope, S. J. A. *New J. Chem.* **2008**, *32*, 1097−1102.

(22) Thorp-Greenwood, F. L.; Fernandez-Moreira, V.; Millet, C. O.; Williams, C. F.; Cable, J.; Hayes, A. J.; Lloyd, D.; Coogan, M. P. *Chem. Commun.* **2011**, *47*, 3096−3098.

(23) Coogan, M. P.; Fernandez-Moreira, V.; Hess, J. B.; Pope, S. J. A.; Williams, C. *New J. Chem.* **2009**, *33*, 1094−1099.

(24) Wrighton, M. S.; Morse, D. L. *J. Am. Chem. Soc.* **1974**, *96*, 998−1003.

(25) Fredericks, S. M.; Luong, J. C.; Wrighton, M. S. *J. Am. Chem. Soc.* **1979**, *101*, 7415−7417.

(26) Rajput, L.; Biradha, K. *New J. Chem.* **2010**, *34*, 2415−2428.

(27) (a) Jones, J. E.; Kariuki, B. M.; Ward, B. D.; Pope, S. J. A. *Dalton Trans.* **2011**, *40*, 3498−3509. (b) Mullice, L. A.; Pope, S. J. A. *Dalton Trans.* **2010**, *39*, 5908−5917.

(28) Wallace, L.; Rillema, D. P. *Inorg. Chem.* **1993**, *32*, 3836−3834.

(29) Thorp-Greenwood, F. L.; Coogan, M. P.; Hallett, A. J.; Laye, R. H.; Pope, S. J. A. *J. Organomet. Chem.* **2009**, *694*, 1400−1406.

(30) Kato, S. I.; Nonaka, Y.; Shimasaki, T.; Goto, K.; Shinmyozu. *J. Org. Chem.* **2008**, *73*, 4063−4075.

(31) Shanze, K. S.; MacQueen, D. B.; Perkins, T. A.; Cabana, L. A. *Coord. Chem. Rev.* **1993**, *122*, 63−89.

(32) Balan, B.; Gopidas, K. R. *Chem.—Eur. J.* **2007**, 5173−5185.

(33) Thornton, N. B.; Schanze, K. S. *Inorg. Chem.* **1993**, *32*, 4994−4995.

(34) Thornton, N. B.; Schanze, K. S. *New J. Chem.* **1996**, *20*, 791−800.

(35) Pawlet, J. B., Ed.; *Handbook of Biological Confocal Microscopy*; Springer: New York, 2006.

(36) A series of Z-stack scans showing the nucleolar localization of **Re2-phen-L3** can be viewed as the original Z-stack series with LCS Lite available free at ftp://ftp.llt.de/softlib/LCSLite/LCSLite2611537.exe and can also be viewed as single images with a variety of image handling software.